Geophys. J. Int. (1999) **139,** 248–260

The thermal evolution of sedimentary basins and its effect on the maturation of hydrocarbons

Filippo Palumbo,[1,2] Ian G. Main[1] and Giammaria Zito[2]

[1] *Department of Geology and Geophysics, University of Edinburgh, Grant Institute, West Mains Road, Edinburgh* EH9 3JW, *UK*
[2] *Dipartimento di Geologia e Geofisica–Universitá degli Studi di Bari, Via Orabona no.* 4, 70125 *Bari, Italy*

Accepted 1999 February 18. Received 1999 January 25; in original form 1997 July 18

SUMMARY

The maturation of hydrocarbon source rocks depends on a range of factors, including the primary rock type and its original content of organic matter (kerogens); the history of sedimentation and burial (depth); the local geothermal gradient (temperature); and duration of sedimentation (time). The standard approach to modelling this process assumes an evolving burial history, but in a basin with a steady-state geotherm, both in the sediment column and in the underlying basement rocks. This first-order approach neglects any effects of changes in the geothermal profile resulting from the timing and history of the particular mechanism that formed the sedimentary basin, and hence may lead to systematic overestimation or underestimation of hydrocarbon maturation in such rocks. This systematic effect may be small when sedimentation rates are low, but can be significant in basins with sedimentation rates that are rapid when compared with the rate of heat transport and re-equilibration in the system.

Here we describe two analytical 1-D mathematical models for diffusive heat transport during sediment deposition, which is rapid compared with the thermal relaxation rate. The two models describe sedimentary events that can be considered either effectively instantaneous (sudden) or continuous. In both cases we calculate a time-dependent geothermal profile and the resulting maturation index of particular source rocks, given the combined effects of the thermal and burial histories. The models take account both of the transient cooling effect of the cold sediment blanket and of the steady-state warming from the underlying basement. After calibration with borehole data, the method allows a reconstruction of the initial geothermal gradient at the start of the sedimentation event.

The model has been applied to data derived from two wells drilled in two different tectonic settings: the Pannonian Basin and the Central North Sea. In both cases there is a good agreement between the model predictions of the maturation index and empirical observations based on the vitrinite reflectance technique applied to borehole samples of actual source rocks. In contrast, the steady-state geotherm models give a systematic overestimation of both the maximum temperature and the degree of maturation reached by the sediments by the end of the sedimentary event; this overestimation is particularly evident for the case of the Pannonian Basin. Such systematic effects could have significant implications both for the interpretation of past thermotectonic events, and for oilfield appraisal.

Key words: geothermics, maturation of hydrocarbons, sedimentation.

1 INTRODUCTION

The main aim of this work is to develop an analytical method to predict the effect of the evolution of the Earth's thermal profile on the maturation of hydrocarbons in a sedimentary basin. This is important because the combined effects of sedimentary processes and heat flow are the prime control on the rate and extent of hydrocarbon maturation in potential source rocks, which is of prime interest in oilfield appraisal. The technique, when calibrated against oilfield data on the maturation of hydrocarbons in potential oil source rocks, can then be used to infer the past geothermal gradient, and hence the conditions at the onset of burial and sedimentation in thermotectonic events involving sedimentation.

The maturation of hydrocarbons involves the slow thermodynamic conversion of organic matter (*kerogens*) in potential source rocks into oil and gas, which may then migrate to more porous reservoir rocks. The maturation process is heavily influenced by two factors: the local temperature; and the duration of the thermal event. In turn, these are strongly controlled by the rates of subsidence and sedimentation. During basin-forming events, large amounts of heat are transferred from the basement through the evolving sedimentary cover, providing an energy source for the maturation process. As in any 'slow cooking' process, however, maturation can occur at a given temperature only if the *effective heating time* is long enough. The *maturation index*, which depends on both the effective heating time and the thermal history, is a quantitative measure of the degree of maturation. It is common practice to simplify the mathematical problem by assuming a time-independent geothermal gradient, so that sediments are heated at a rate that depends only on the depth of burial, and hence only on the burial history (i.e. source rock depth as a function of time). In this work we evaluate the effect of a realistic time-dependent geothermal gradient on the thermal history and the resulting maturation index, and apply our model to two end-member examples of subsidence and sedimentation based on borehole data.

A number of models have been proposed to describe quantitatively the relationship between thermal history and organic maturity since the first attempt by Karweil (1956), and the subject is now included in elementary textbooks (e.g. North 1985). Tissot (1969) proposed the first mathematical model for oil generation using the Arrhenius kinetic theory, calculated along a time–depth curve representing the burial history of a source rock. However, the most widely applied models are the quartet of Bostick (1973), Hood *et al.* (1975), Lopatin (1976) and Waples (1980). Vetö & Dövényi (1986) compared the performances of these four methods, using data collected from boreholes in oilfields all over the world. They conclude that the model of Waples (1980) gives the best statistical match to the observed *vitrinite reflectance*, R_o (a quantitative optical measure of the degree of maturation). This is commonly found to be in the range $0.2 \leq R_o \leq 2.0$ for potential hydrocarbon source rocks, but significant hydrocarbons are produced only from rocks with vitrinite reflectance in the range $0.65 \leq R_o \leq 1.30$. The former range for the vitrinite reflectance, and its associated range of maturation index after calibration, is known as the *oil generative window*. The vitrinite reflectance technique, because of its simplicity, is still in common use by geologists for a quick estimation of the degree of maturation in the organic content of potential source rocks (Pieri 1988; Cranganu & Deming 1996).

However, these widely applied models for maturation account only for the burial history, and assume a background constant geothermal gradient G. The models therefore neglect the feedback effect of the sedimentary process itself on the local thermal gradient, where cool sediments are laid down upon a background geothermal gradient in the basement rocks. The result of this 'cold blanketing' effect is to depress the isotherms within the sediment column with respect to the constant G model, and to introduce a transient cooling of the basement, which then gradually recovers to the background geothermal gradient with a characteristic relaxation time that depends on the average thermal diffusivity of the sediment column, the sediment thickness, and its rate of deposition. Here we develop an analytical model which explicitly takes account of the effect of these processes on the geothermal profile.

An example of a model with a constant geothermal gradient is shown in Fig. 1 (after Waples 1980). This figure shows a complicated history of burial and uplift for three sedimentary layers overlying the initial basement. The thin, middle sedimentary layer is the potential source rock in this diagram. The geothermal gradient is assumed constant, so the dashed isotherms are precisely horizontal. The maturation index, shown in contours on the diagram, is the time temperature index (denoted TTI as shown in the diagram), defined by

$$TTI = \sum_{n_{\min}}^{n_{\max}} r^n \Delta t_n \qquad (1)$$

(Waples 1980). Δt_n is the time interval (in Ma) that the rock spent in the nth temperature interval, usually split into 10 °C bands, $n_{\min}$ and $n_{\max}$ are the minimum and maximum values of the index n, and r is an arbitrary number describing the exponential dependence (see North 1985, p. 59). This model assumes that the maturation rate is exponential in temperature and linear in time for a particular interval of temperature and time—both are reasonable assumptions. After empirical calibration tests, the optimum value for the factor r is found to be $r = 2$ (Waples 1980).

Typically, hydrocarbons are produced for time–temperature indices in the range $15 < TTI < 160$. After calibration, this corresponds to a range of $0.65 \leq R_o \leq 1.30$ for the oil generative window determined by the vitrinite reflectance technique. For values lower than the threshold value of $TTI = 15$ no hydrocarbons are produced, and for values higher than 160 all of the oil has been expelled from the source rock. In addition, there is another threshold value of $TTI = 75$, which corresponds to the peak of maturation reached by the organic matter within the source rock. The oil generative window corresponds to the intersection on Fig. 1 of the burial curve for the source rock with the appropriate range of the time–temperature index for maturation. This area is highlighted in black in Fig. 1.

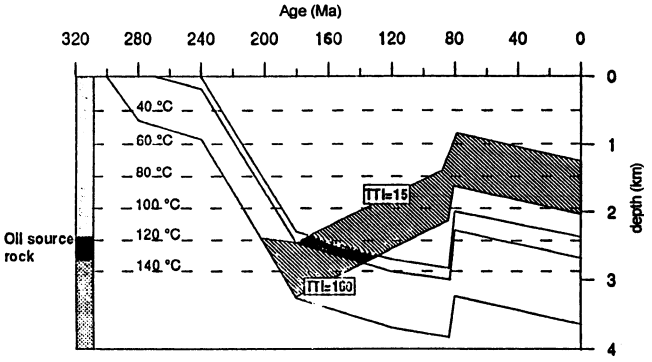

Figure 1. Isomaturity lines on a geological reconstruction, according to the constant geotherm method of Waples (1980). The x-axis shows the age of the deposited sediments, and the y-axis shows the depth of the sediments. The dashed lines represent the isotherms during time, assumed constant. The shaded region denotes the oil generative window, described in the text, while the black region shows the path of the source rocks involved in the process of maturation, through the oil generative window. The present-day stratigraphic column (adapted from Pieri 1988), is outlined on the left.

2 THEORETICAL MODELS

In order to allow an analytical solution to the problem of time-dependent heat transfer, the methods presented here still make some simplifying assumptions. In particular, we assume that the effects of a more complex sedimentary history on the evolving geothermal profile (for example the stepwise constant burial rates in the discrete sedimentation events shown in Fig. 1) can be accounted for to first order by applying an average sedimentation rate and average thermal diffusivity for the sedimentary column. Although this may be a reasonable assumption for many cases, there will be some cases of episodic sedimentation where this will not apply.

As a first-order approximation, we consider a constant background geothermal gradient in the basement rock. Our main concern here is to determine the first-order effect of the sediment blanket on the geothermal profile, using analytical techniques that allow us to evaluate the effect of the model parameters directly. Numerical methods could be used, but the analytical solution gives more accurate results. The analytical approach also allows a sensitivity analysis of the main controlling variables to be carried out, before we progress to the more general case, which will require the application of numerical methods. We first describe the analytical model, and then apply it to two case studies of hydrocarbon maturation in sedimentary basins where the simplifying assumptions can be justified.

In this section we derive a mathematical model for the time-dependent evolution of isotherms in a sedimentary basin. Once this history is known, it is then straightforward to apply standard methods (e.g. Waples 1980) to calculate the maturation index for the source rocks, given independent constraints on the boundary conditions of the basin or borehole we wish to investigate. Sedimentation is always accompanied by subsidence: consequently, the isotherms initially shift systematically downwards compared with the initial geothermal gradient (as in Fig. 2a). When subsidence is over, the isotherms tend to relax upwards to reach the steady state asymptotically. If the sedimentation rate is slow compared with the rate of thermal relaxation which in turn depends on the average thermal diffusivity of the sediments, burial rate and sedimentary thickness), then the assumption of a constant geothermal gradient (e.g. Fig. 1) is adequate. If the sedimentation rate is rapid compared with this thermal relaxation rate, however, then we must explicitly take the transient effect into account (e.g. Fig. 2a). We now describe mathematical models for two analytically tractable cases of relatively rapid sedimentation which are effectively either instantaneous (Section 2.1) or continuous, at a constant but finite rate (Section 2.2).

2.1 Instantaneous sedimentation

If the subsidence, and consequently the sedimentation, is so rapid geologically that it can be treated as effectively instantaneous, then the initial temperature in the whole sediment column is equal to that at the sediment surface, the geothermal gradient in the sediment column is zero, and the geothermal profile within the basement is unchanged (Fig. 3). This profile then relaxes to the final geothermal gradient by heat transfer from below, at a rate determined by the initial conditions and the thermal diffusivity of the sediments.

The generic problem we will solve here is that of vertical heat conduction in a 1-D semi-infinite solid. More complex geology and tectonics involving lateral heat transport are neglected, so our model applies most closely to the centre of sedimentary basins rather than the edges. These edge effects could be modelled by more complex finite difference models in three dimensions where appropriate. The generic equation for 1-D thermal diffusion is

$$\frac{\partial^2 T}{\partial z^2} = \frac{1}{\kappa}\frac{\partial T}{\partial t}, \tag{2}$$

where T is the temperature, z is the depth, t is time, and κ is the thermal diffusivity.

The effect of instantaneous sedimentation can be calculated assuming that suddenly, at $t = 0$, a uniform layer of thickness H is deposited on the seafloor. The following initial and boundary conditions can be used to describe such a sudden sedimentation:

(1) $t = 0, \quad T = T_o \quad 0 \le z \le H,$

$\quad T = T_o + G(z - H) \quad z > H.$

(2) $t > 0 \quad T = T_o \quad z = 0.$

The solution of eq. (2) under these boundary conditions is

$$T(z,t) = T_o + \frac{1}{2\sqrt{\pi\kappa t}}\int_H^\infty G(z' - H) \times \left\{\exp\left[-\frac{(z-z')^2}{4\kappa t}\right] - \exp\left[-\frac{(z+z')^2}{4\kappa t}\right]\right\} dz', \tag{3}$$

where κ is the average thermal diffusivity of the sedimentary column. For $0 \le z \le H$ the expression (3) can be written (according to Birch *et al.* 1968 and Mongelli 1981) as

$$T(z,t) = T_o + Gz + G(\sqrt{\kappa t})\left[\text{ierfc}\left(\frac{H-z}{2\sqrt{\kappa t}}\right) - \text{ierfc}\left(\frac{H+z}{2\sqrt{\kappa t}}\right)\right], \tag{4}$$

Figure 2. (a) Schematic representation of the evolution of the isotherms during a continuous sedimentary event. The x-axis shows the age of the deposited sediments, and the y-axis shows the depth of the sediments. The shaded region represents the rock basement on which the sediments are accumulating. The dashed straight lines represent the isotherms during time according to a steady geothermal gradient, while the solid curved lines represent the evolution of the isotherms according to our time-dependent model. (b) Maturation history during the continuous deposition (case in part a) of a pack of sediments at a rate of 40 km Ma^{-1}, on a basement with an initial geothermal gradient of 30 °C km^{-1}. The mean thermal diffusivity of the whole system is 31.54 km^2 Ma^{-1}. The sediments forming our hypothetical sedimentary column are shown on the right. (c) Comparison of the predicted oil generative window obtained for the case of part (a), for the two models. The dashed area represents the oil generative window for a constant geothermal gradient, while the backward slashed area represents the oil generative window for a geothermal gradient that varies over time.

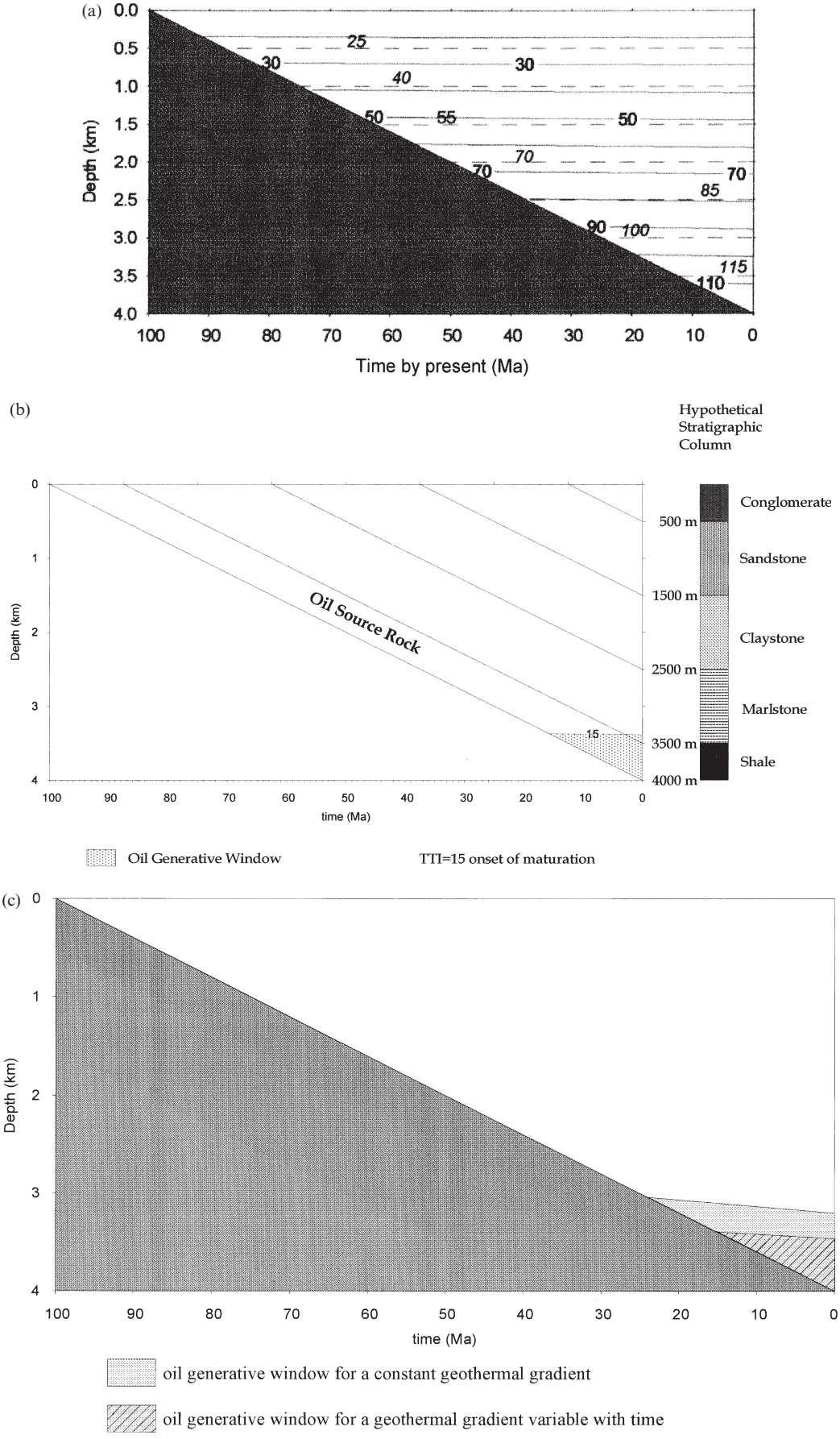

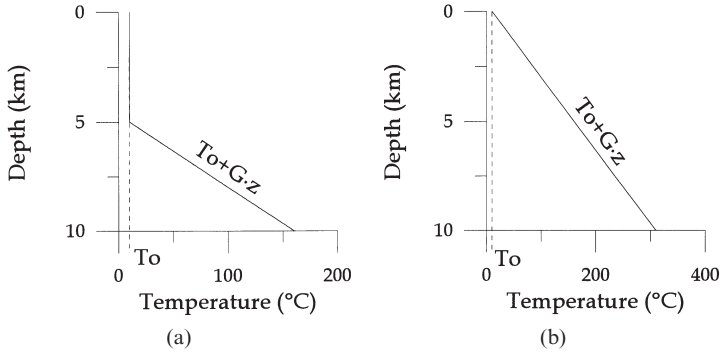

Figure 3. The initial thermal profiles for the two types of sedimentation discussed here. (a) represents the initial thermal profile for a sudden sedimentation, while (b) represents the initial thermal profile for a continuous sedimentation. The x-axis shows the temperature (in °C). The y-axis shows the depth (in km).

where ierfc(x) is the first integral of the complementary error function. Here we prefer to recast this equation in terms of the error function erf(x), because this function is easier to manage from a computational point of view. Eq. (4) can be recast in the following form:

$$T(z,t) = T_o + Gz + G \left[\left(\frac{H-z}{2} \right) \mathrm{erf}\left(\frac{H-z}{2\sqrt{\kappa t}} \right) - \left(\frac{H-z}{2} \right) \mathrm{erf}\left(\frac{H+z}{2\sqrt{\kappa t}} \right) \right] + G\sqrt{\frac{\kappa t}{\pi}} \left\{ \exp\left[-\left(\frac{H-z}{2\sqrt{\kappa t}} \right)^2 \right] - \exp\left[-\left(\frac{H+z}{2\sqrt{\kappa t}} \right)^2 \right] \right\}. \quad (5)$$

2.2 Continuous sedimentation

The effects of a finite sedimentation rate are important in the intermediate case where sedimentation is too slow to be considered instantaneous, but still too fast to justify the assumption of a constant geothermal gradient. An example of this case has already been illustrated in Fig. 2(a), using an example calculated from the methods described below for the case of a single episode of continuous sedimentation at a steady rate. In this figure we can observe the blanketing effect of sedimentation, which depresses the isotherms in the sedimentary column (solid curves). The dashed straight lines on the diagram, representing the assumption of a constant geothermal gradient, have been added for comparison. Fig. 2(b) shows the maturation history, calculated from the data shown in Fig. 2(a), for steady-state sedimentation at a constant rate of 40 m Ma^{-1}, starting at 100 Ma BP, for a hypothetical stratigraphic column with an average thermal diffusivity of 31.54 $km^2\ Ma^{-1}$. We compared the time-dependent and time-independent maturation histories for this hypothetical sedimentary column, assuming a constant initial geothermal gradient of $G = 30$ °C km^{-1}, all other variables being held constant. For the present time in this hypothetical simulation, Table 1 gives the predicted values at the bottom of the sedimentary column (depth of 4 km) for the maximum temperature, T_{max}, the Time–Temperature Index, TTI, and vitrinite reflectance, $\%R_o$.

Table 1. The maximum temperature T_{max} and the time-temperature index TTI calculated for the present time at the bottom of a hypothetical sedimentary column for the model with a constant geothermal gradient and our model with an initial geothermal gradient evolving during the sedimentation. Calculations are for a column deposited at a rate of 40 m Ma^{-1}, starting 100 Myr ago, with an average thermal diffusivity of 31.54 $km^2\ Ma^{-1}$ and initial geothermal gradient of 30 °C km^{-1}; see Fig. 2a.

	T_{max} (°C)	TTI	$\%R_o$
For G constant	130	66	0.96
For G variable	121	41	0.85

This table illustrates the clear overestimation of all parameters, particularly the maturation index, associated with the assumption of a constant geothermal gradient. This overestimation is clearly shown in Fig. 2(c), in which we can compare the oil generative window for a time–independent maturation history (dashed area) with that for a time–dependent maturation history (backward slashed area). Fig. 2(b) highlights the oil generative window for a hypothetical source rock within the sedimentary column. In this case the maturation process, for the sediments at the bottom of the sedimentary column, starts at 15.725 Ma BP, while at the present time the thermal conditions for the maturation process are reached at 3385 m depth. Therefore at the present time the whole oil source layer is involved in the maturation process.

The problem of continuous sedimentation belongs to the class of heat conduction problems in a semi-infinite solid, with a boundary that moves at a finite velocity u_z along the z-axis. In our case, u_z is positive; that is, it corresponds to an accreting medium (analogous to a snowfield which is being supplemented at a steady rate—for example Carlsaw & Jaeger 1959). This means that, if material is accreted at the surface by sedimentation, the material below can be regarded as moving away from the surface at a constant rate (Mongelli 1981). The 1-D diffusion equation for the case of a moving boundary is

$$\frac{\partial^2 T}{\partial z^2} - \frac{u_z}{\kappa}\frac{\partial T}{\partial z} - \frac{1}{\kappa}\frac{\partial T}{\partial t} = 0. \quad (6)$$

The following initial and boundary conditions apply in this case:

$$(1)\ t=0, \qquad T(z)=T_o+Gz, \qquad z\geq 0;$$

$$(2)\ t>0, \qquad T=T_o, \qquad z=0.$$

The solution of eq. (6) can be obtained using the Laplace transformation method, by considering the following subsidiary equation:

$$\frac{\partial^2 \bar{T}}{\partial z^2}-\frac{u_z}{\kappa}\frac{\partial \bar{T}}{\partial z}-\frac{p}{\kappa}\bar{T}=-\frac{T_o+Gz}{\kappa}, \tag{7}$$

where $\bar{T}$ is the subsidiary variable and p is the parameter used for the Laplace transformation. The solution of (6) and (7) under the stated boundary conditions is

$$T(z,t)=T_o+G(z-u_z t)+\frac{1}{2}G\left[(z+u_z t)\exp\left(\frac{u_z z}{\kappa}\right)\operatorname{erfc}\left(\frac{z+u_z t}{2\sqrt{\kappa t}}\right)-(z-u_z t)\operatorname{erfc}\left(\frac{z-u_z t}{2\sqrt{\kappa t}}\right)\right], \tag{8}$$

where $\operatorname{erfc}(x)$ is the complementary error function, u_z is the mean sedimentation rate along the z-axis, and κ is the average thermal diffusivity (Carslaw & Jaeger 1959).

The two mathematical expressions, (5) and (8), can be used to calculate the thermal evolution with respect to time of a sedimentary layer, depending on their respective limits of applicability.

It is then straightforward to evaluate the effects of the thermal correction on the maturation index for the basin, and compare this with the observed value. Similarly, the effect of the other variables that affect the system, such as the initial geothermal gradient and the thermal diffusivity, can be determined in a straightforward way. In the general case a full numerical solution would be required.

3 SENSITIVITY ANALYSIS

One of the advantages of the analytical approach is the potential to carry out a sensitivity analysis of the key variables. In this section, we describe the results for several theoretical cases, to examine how the major variables determine the evolution of the system under different conditions. For example, Figs 4 and 5 show curves for the onset time of maturation, for various initial geothermal gradients (Fig. 4) and mean thermal diffusivities (Fig. 5), in the case of sudden sedimentation. In Fig. 4, we notice that none of the sediments in this example will be involved in the maturation process if the initial geothermal gradient is less than 24.8 °C km^{-1}. By developing graphs like this one, we can predict when the maturation process should begin at any particular depth as the sedimentary blanket heats up. A similar calculations can also be made for the peak and the end of the maturation process. For example, in Fig. 4 none of the sediments will reach the peak

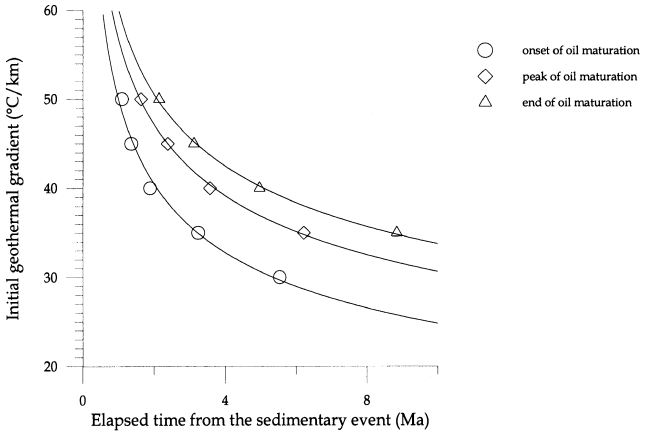

Figure 4. Curve of the best fit for the onset, peak and end of maturation at the bottom of a hypothetical sedimentary column 5 km thick, having a mean thermal diffusivity of 35.66 km^2 Ma^{-1} and suddenly deposited 10 Ma ago. The x-axis shows the time from the sedimentary event in millions of years, and the y-axis represents the initial geothermal gradient.

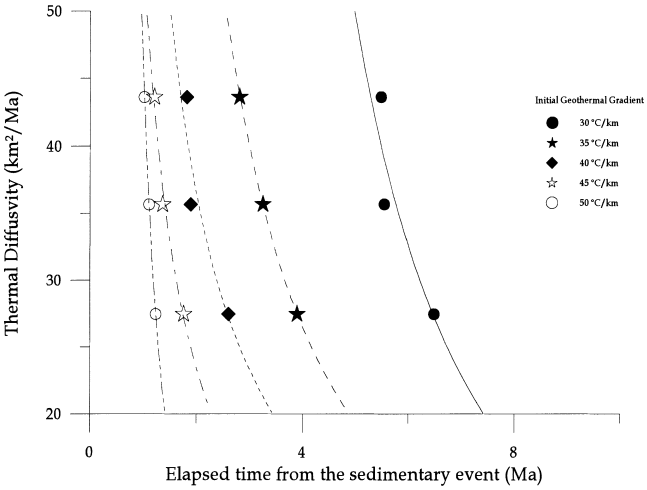

Figure 5. Curves of the best fit for the onset of the maturation, for sediments at the bottom of a 5 km thick layer, for various values of the initial geothermal gradient. The x-axis shows the elapsed time from the sedimentary event. The y-axis shows the thermal diffusivity.

of oil maturation if the initial geothermal gradient is less than 30.7 °C km^{-1}, and none of the sediments will pass through the whole maturation process unless the initial geothermal gradient is greater than 33.7 °C km^{-1}. An example of the dependence of the onset of the maturation on the thermal diffusivity is shown in Fig. 5. Again, similar calculations can be carried out for the peak and the end of the maturation. For a given intial geothermal gradient, and a given depth, we predict an earlier start of the maturation process with increasing κ. As the initial gradient increases, however, the difference between the onset of the maturation for high values of κ and low values of κ becomes smaller.

The same kind of analysis has been carried out for the case of continuous sedimentation. The trend of the isotherms in a

continuously subsiding basin is for them to bend downwards with ongoing sedimentation (Fig. 2a). This depression of the isotherms is due to the cooling effect of the sedimentation. The oil generative window tends to reach shallower depths with increasing time, increasing thermal diffusivity, increasing sedimentation rate, and increasing initial geothermal gradient. For example, in Fig. 6 we can see how the oil generative window evolves with increasing initial geothermal gradient for a given sedimentary event, calculated at a given time (the 'present' time in the simulations). Fig. 6 demonstrates that the maturation process does not occur during steady sedimentation if the initial gradient is less than 25 °C km^{-1}. From the results obtained, we conclude that the effect of the thermal diffusivity on the system is less significant than the effect of time or, more importantly, than the effect of the thermal state of the basement on which the sediments are accumulating. For this reason our model can be used to some extent as a geothermometer; that is, if we know the correct, present-day geothermal gradient and the sedimentary history of a basin (timing and lithologies), in principle we can recover the thermal state of that area at the onset of sedimentation. This is illustrated below for two individual case studies representing instantaneous and continuous sedimentation.

As stated in the Introduction, previous models to evaluate the maturation index were based on the assumption that the geothermal gradient is constant for the whole duration of the sedimentation (e.g. Hood *et al.* 1975; Waples 1980; North 1985; Pieri 1988; Hunt 1995). For the case illustrated in Fig. 2, this static assumption leads to a significant difference in results compared to evolutionary model. Further examples were run using the same technique to calculate the time–temperature index in both cases. We considered the same depositional history (i.e. the same sedimentation rate and the same time of sedimentation) and the same average thermal diffusivity for the whole system. The geothermal gradient (constant in the first case and initial in the second case) is 30 °C km^{-1}. Table 2 summarizes the results.

It is clear that both T_{max} and TTI_{max} can be greatly overestimated if we assume a constant geothermal gradient: for example, in case 2 of Table 2 the sediments at the bottom of the sedimentary column are postmature for constant G, while they are still in the catagenetic phase for variable G. In Fig. 7, we compare the results graphically for Case 1. Hence, the results arising from this section demonstrate that the neglect of the thermal evolution of basins can result in a significant overestimation of the TTI. This overestimation increases with increasing geothermal gradient.

In the next section we will apply our models to some real data sets, in order to evaluate the thermal histories and their effects on the oil generative window.

4 CASE STUDIES

In order to illustrate the effect of the changing geothermal gradient on the relevant calculations, we now apply our models to two real cases of sedimentary basins, representing type

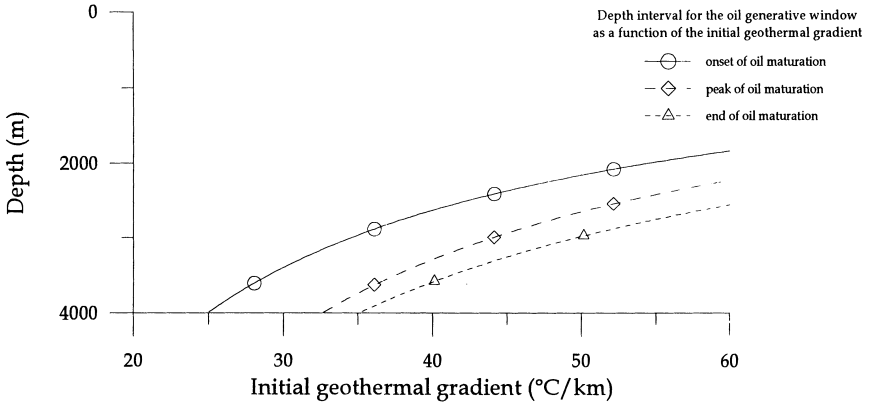

Figure 6. Plot of depth intervals for the hydrocarbon maturation in a continuous event (beginning at 100 Ma at a steady rate of 40 m Ma^{-1} and with a mean thermal diffusivity of 31.54 km^2 Ma^{-1}) at the present time, as a function of initial geothermal gradient. The x-axis shows the initial geothermal gradient, and the y-axis represents the maximum depth of the sediments at the present time.

Table 2. The time–temperature index, calculated from eq. (1) with $r = 2$, for a model with a constant geothermal gradient and for a model with a geothermal gradient which evolves during the sedimentation, at the bottom of the stratigraphic column at the present time. Calculations are for a sedimentary layer ($H = 4$ km) deposited over a time interval of 100 Ma at a burial rate of 40 m Ma^{-1}, under various initial thermal conditions (different geothermal background gradients). We consider that the temperature at the seafloor is $T_o = 10$ °C.

	Initial geothermal gradient G (°C km^{-1})	T_{max} for a constant gradient in the deposited sediments (°C)	T_{max} for a time-dependent geothermal gradient in the deposited sediments (°C)	TTI_{max} for G constant	TTI_{max} for a time-dependent G
Case 1	30	130	121	66 (=0.96%R_o)	41 (=0.96%R_o)
Case 2	35	150	139	229 (=1.42%R_o)	124 (=1.20%R_o)
Case 3	40	170	158	800 (=1.95%R_o)	401 (=1.65%R_o)
Case 4	45	190	174	2844 (=2.52%R_o)	1312 (=2.14%R_o)
Case 5	50	210	195	10 240 (=3.35%R_o)	4289 (=2.78%R_o)

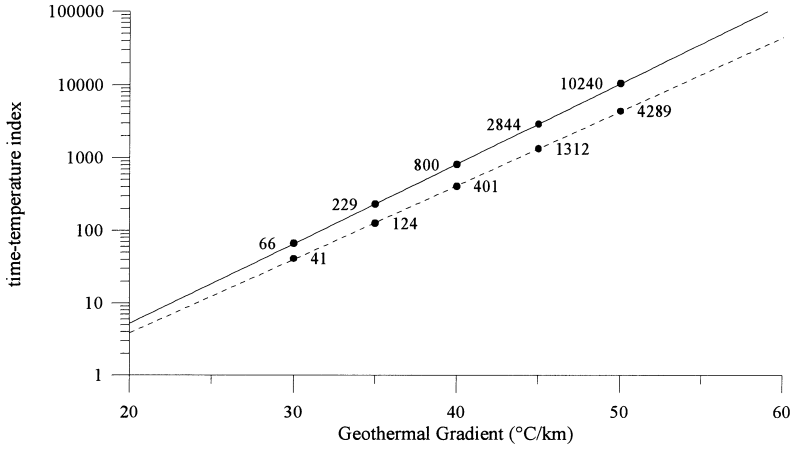

Figure 7. Comparison between the predicted values of the time–temperature index of Table 2. The solid line represents the values obtained for a constant geothermal gradient, while the dashed line represents the values obtained according to our time-dependent model. The *x*-axis shows the geothermal gradient (constant and initial for the two models respectively) in $^{\circ}C\,km^{-1}$, and the *y*-axis (plotted on a logarithmic scale to facilitate the presentation of the data) shows the time–temperature index. The labels indicate the values of *TTI* for each of the cases in Table 2.

examples of the two sedimentation processes described in Section 2. These are (Section 4.1) the Romanian section of the Pannonian Basin and (Section 4.2) the Central North Sea. The first case can be treated as an example of instantaneous, recent sedimentation, while the latter must be treated as an example of continuous and older sedimentation, extending to the present day. We evaluate their actual thermal and maturation histories, calibrated by geophysical and lithological well logs derived from borehole data.

4.1 The Pannonian Basin

The Neogene structure of the sector of the Pannonian Depression considered here (shown in Fig. 8) is based on seismic and borehole data (Visarion *et al.* 1979). The basin is characterized by a brittle style of deformation, with faults forming a graben–horst-like structure. The Hódmezóvásárhely-I (Hód-I) borehole used here is located in southeast Hungary, in a Neogene sedimentary trough. Its bottom depth is 5842.5 m,

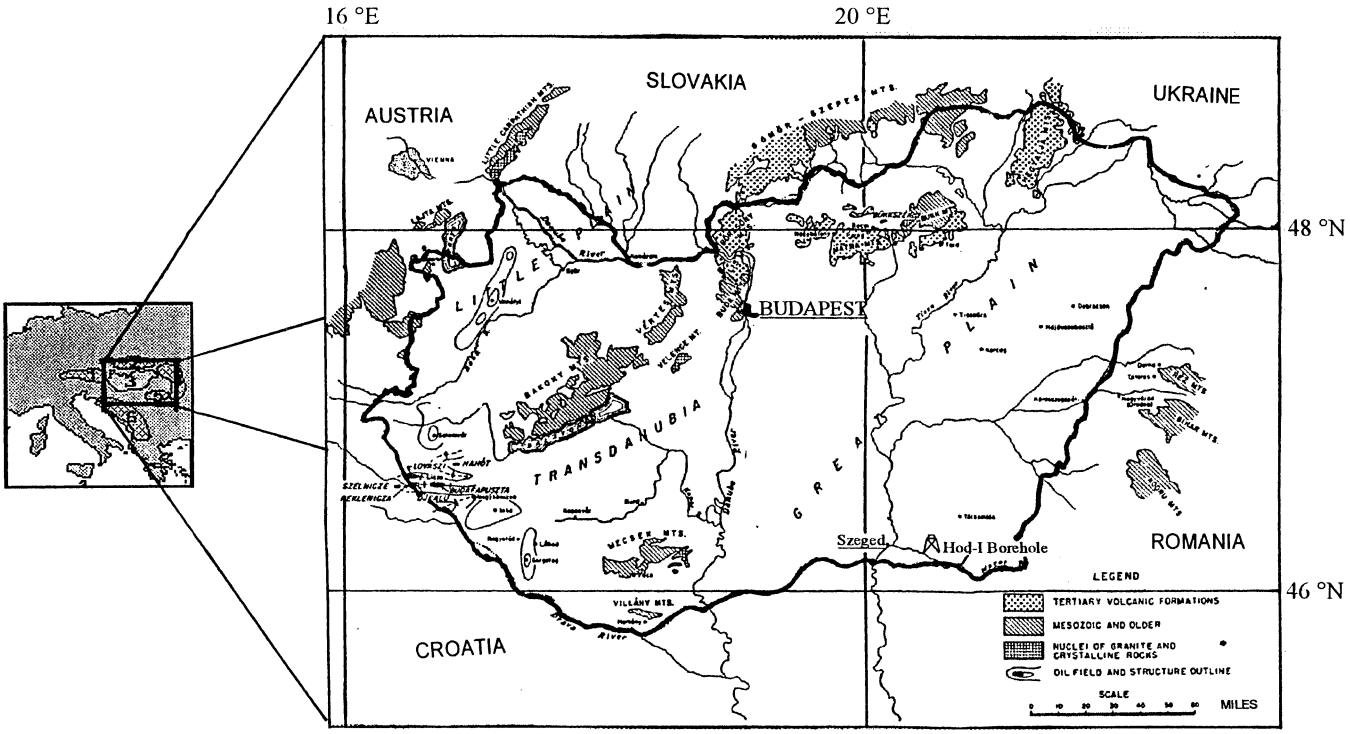

Figure 8. Localization of the Hód-I borehole. The small picture on the left shows the location of the considered area. (1) Eastern Alps, (2) Western Carpathians, (3) Pannonian Basin, (4) Eastern Carpathians, (5) Southern Carpathians, (6) Dinarides (from Vajk 1953).

occurring within sedimentary rocks of Badenian (Middle Miocene) age (Sajgó *et al.* 1988). The mid-Miocene bottom depth, corresponding to a maximum age of sedimentation of 15.5 Ma, and is just within the window for the validity of the assumption of effectively instantaneous sedimentation. The borehole data (rock type and sedimentary thickness) were used, in conjunction with published thermal diffusivity data, to reconstruct an average thermal diffusivity in the sediment column of 18.35 $km^2\,Ma^{-1}$ (a thickness-weighted arithmetic mean, after Oliva & Terrasi 1976). The total sediment thickness, H, was taken to be the depth of the base of the borehole. No independent data were available for the local geothermal gradient, so an initial geothermal gradient of 39.5 $°C\,km^{-1}$ was obtained by trial and error, based on calibration with the observed maturation index for oil source rocks as described below.

The resulting thermal relaxation and maturation (TTI) curves are shown in Fig. 9. The theoretical isotherms are computed using eq. (5), together with the isomaturity curves representing the oil generative window calculated using the method of Waples (1980). In Fig. 9 we assume that all of the rocks in the sediment column are potential source rocks. The isomaturity curve for $TTI = 75$ is also shown, because this is the best estimate of the peak of oil maturation (Waples 1980). From the diagram it can be seen that the isotherms show an asymptotic recovery to the initial geothermal gradient over timescales that depend on the temperature at the top of the basement, ranging from less than 1 Ma just after sedimentation to several million years after 10 Ma of heating from the basement. The thick solid curves for the maturation index (TTI) rise at a constant or decelerating rate, but show no asymptotic behaviour over these timescales, indicating that the maturation process is still ongoing in this area.

From Fig. 9 we can draw the following conclusions.

(1) The onset of the maturation, defined by $TTI = 15$ at the maximum sediment depth of 5842 m, occurs at 12.4 Ma BP, some 3.1 Ma after the initiation of sedimentation in the mid-Miocene. The peak of the maturation ($TTI = 75$ at 5842 m depth) occurred at 10.7 Ma BP, and the end of the maturation process ($TTI = 160$ at 5842 m depth) occurred at 9.36 Ma BP.

(2) At the present time, the predicted depth at which the maturation process is just beginning is 3130 m; the peak of maturation is at 3856 m depth; and the end of the maturation process occurs at 4455 m depth.

These model predictions allow a direct comparison with the results obtained by Stegena (1988), who applied the constant geothermal profile method of Waples (1980) to this borehole.

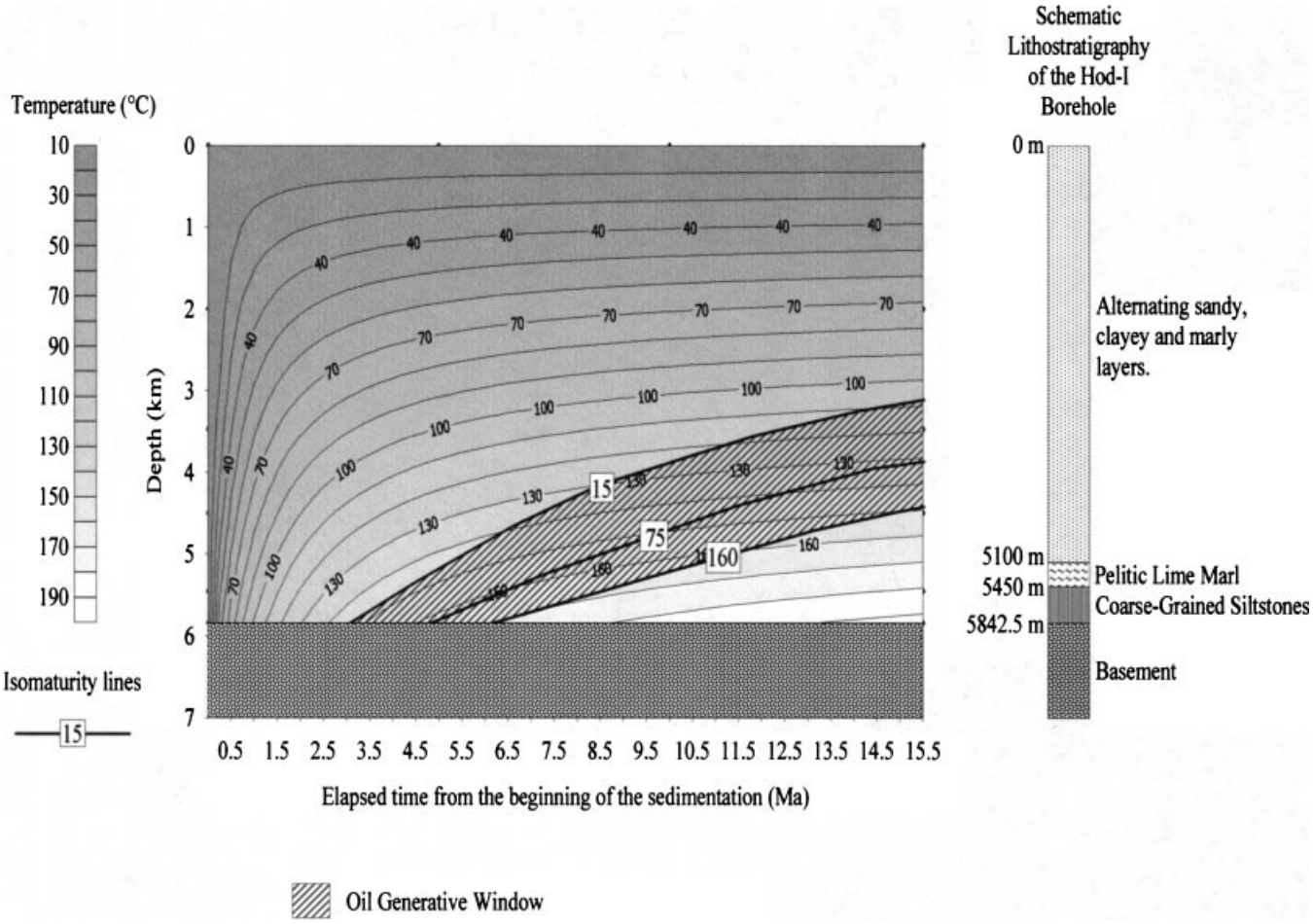

Figure 9. Predicted thermal and maturation history for the Hódmezóvásárhely-I (Hód-I) borehole. The initial geothermal gradient is equal to 39.5 $°C\,km^{-1}$. The mean thermal diffusivity of the deposited sediments is equal to 18.35 $km^2\,Ma^{-1}$. The x-axis shows the time from the beginning of the sedimentation in millions of years, and the y-axis shows the depth in kilometres.

Table 3. The maximum value of the time–temperature index and the corresponding value of the vitrinite reflectance, according to our model for sudden sedimentation, and the two values calculated by Stegena (1988). TTI_{max} is the maximum value of the time–temperature index at the present time at the bottom of the borehole at 5842.5 m depth.

	TTI_{max}	$\%R_o$
Sudden sedimentation (this paper)	2820	2.52
Stegena (constant geothermal gradient) (1988)	8012	3.17
Stegena (heating event at 5 Ma) (1988)	1912	2.32

Stegena (1988) noticed that the predicted vitrinite reflectance using the method of Waples (1980) was too high when compared with the observed value of $TTI = 19$, which corresponds to a value for the vitrinite reflectance of $0.69\%R_o$ at a depth of 3477 m. He therefore obtained a second estimate, taking into account an arbitrary heating event at 5 Ma, for which there is no independent evidence. Our method fits the data adequately without recourse to such an arbitrary event. Table 3 compares our results with the two scenarios calculated by Stegena (1988), using a local calibration for the predicted vitrinite reflectance provided by Sajgó (1988).

This comparison can be pursued further by using the present-day data on vitrinite reflectance obtained independently from source rocks at various depths in the borehole samples (Sajgó *et al.* 1988). From these, we know that the present-day threshold of maturation starts at a depth of 3477 m, where $\%R_o = 0.69$ (corresponding to $TTI = 19$). The predicted value of the vitrinite reflectance from our best-fitting model (Fig. 9) matches this measured value exactly for a geothermal gradient of $39.5\ ^\circ\mathrm{C\ km^{-1}}$. This represents both the initial geothermal gradient of the basement and the equilibrium geothermal gradient of the sedimentary cover. Since the present geothermal gradient ($31.4\ ^\circ\mathrm{C\ km^{-1}}$ for this borehole depth) predicted by the model is quite different from the equilibrium gradient, this means that the cooling effect of the sedimentary cover, like the hydrocarbon maturation, is not yet completed.

In conclusion, the simple model of Waples (1980) fails to fit the observed vitrinite reflectance data adequately in this area. Although the method can be made to fit by introducing an arbitrary thermal event at 5 Ma, there is no independent evidence for such an event (Stegena 1988). However, the observed data can be fitted adequately by the model presented here, using both the observed data and reasonable values for the initial conditions as input.

4.2 The Fisher Bank Basin, Central North Sea

Borehole 22/2-2 is located in the Fisher Bank Basin in the Central North Sea. The North Sea Basin is a Palaeozoic to Holocene multi-stage rift basin within the northwestern European cratonic block, superimposed on the earlier Caledonian orogenic trend (Brigaud *et al.* 1994). The normal-faulted basin structure observed today developed as a result of Permo–Triassic and especially Jurassic rifting (Goff 1983), and its importance in explaining the present-day configuration and structure of the North Sea has been recognized by many authors (e.g. McKenzie 1978). The locations of the main structural features are displayed in Fig. 10. The lithologies are composed predominantly of sands and shales in the

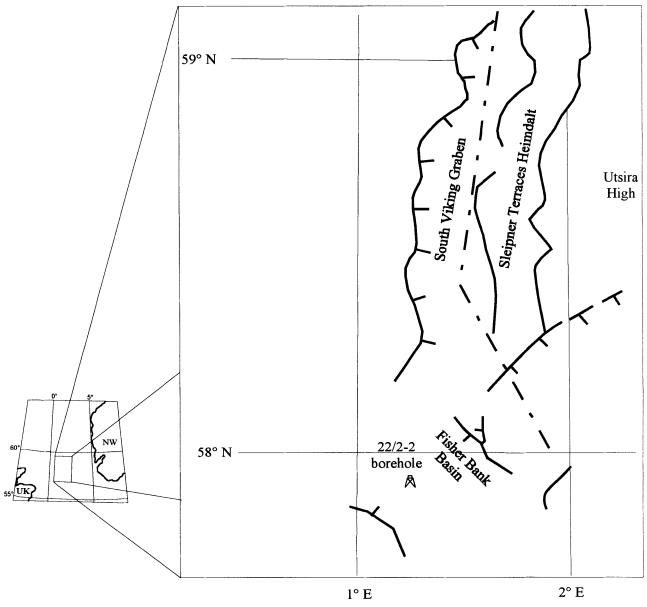

Figure 10. Location of the Moray Firth Arm 22/2-2 borehole [adapted from Brigaud *et al.* (1994) and Turner (1995, personal communication)].

Triassic–Jurassic section of the basin, with organic matter present in source rocks such as the Kimmeridge Clay formation. Cretaceous lithologies are predominantly carbonates and shales, while the Tertiary lithologies are mainly composed of shales, silts and sands (Brigaud *et al.* 1994). The location of Borehole 22/2-2 is also shown in Fig. 10, in an area of intense sedimentation within the North Sea province. The bottom depth of the borehole is located at $H = 6770.732$ m, in sedimentary rocks of Permian age. In this area, sedimentation has been ongoing since the Permian. The time-dependent geothermal profile can therefore be determined using the model that assumes continuous sedimentation, at an average rate that corresponds to $u_z = 23.3\ \mathrm{m\ Ma^{-1}}$.

The weighted average for the thermal diffusivities appropriate for the borehole stratigraphy, again using the method presented in Oliva & Terrasi (1976), is $\kappa = 27.19\ \mathrm{km^2\ Ma^{-1}}$. Assuming a range of starting values for the initial geothermal gradient, we can estimate the thermal and maturation history for this borehole using eq. (8). The results, for the best-fitting initial geothermal gradient of $28\ ^\circ\mathrm{C\ km^{-1}}$, are presented in Fig. 11, which shows (a) the evolving thermal profile, and (b) the burial and maturation history. The oil generative window is highlighted by the hatched area in (b), again assuming source rocks present at all depths. The isotherms are flatter than those in Fig. 9, but are not strictly horizontal as in Fig. 1.

Figs 11(a) and (b) show that the actual burial history is more complicated than that of the assumed model with a constant burial rate, comprising instead a series of discrete events, with different sedimentation rates. The complicated burial curves have a significant effect on the shape of the maturation curves, and have therefore been included in the calculation of the maturation index. However, the effect of smoothing out the burial history for the purpose of calculating the geothermal profile would represent a second-order correction compared with neglecting the sediment blanketing effect.

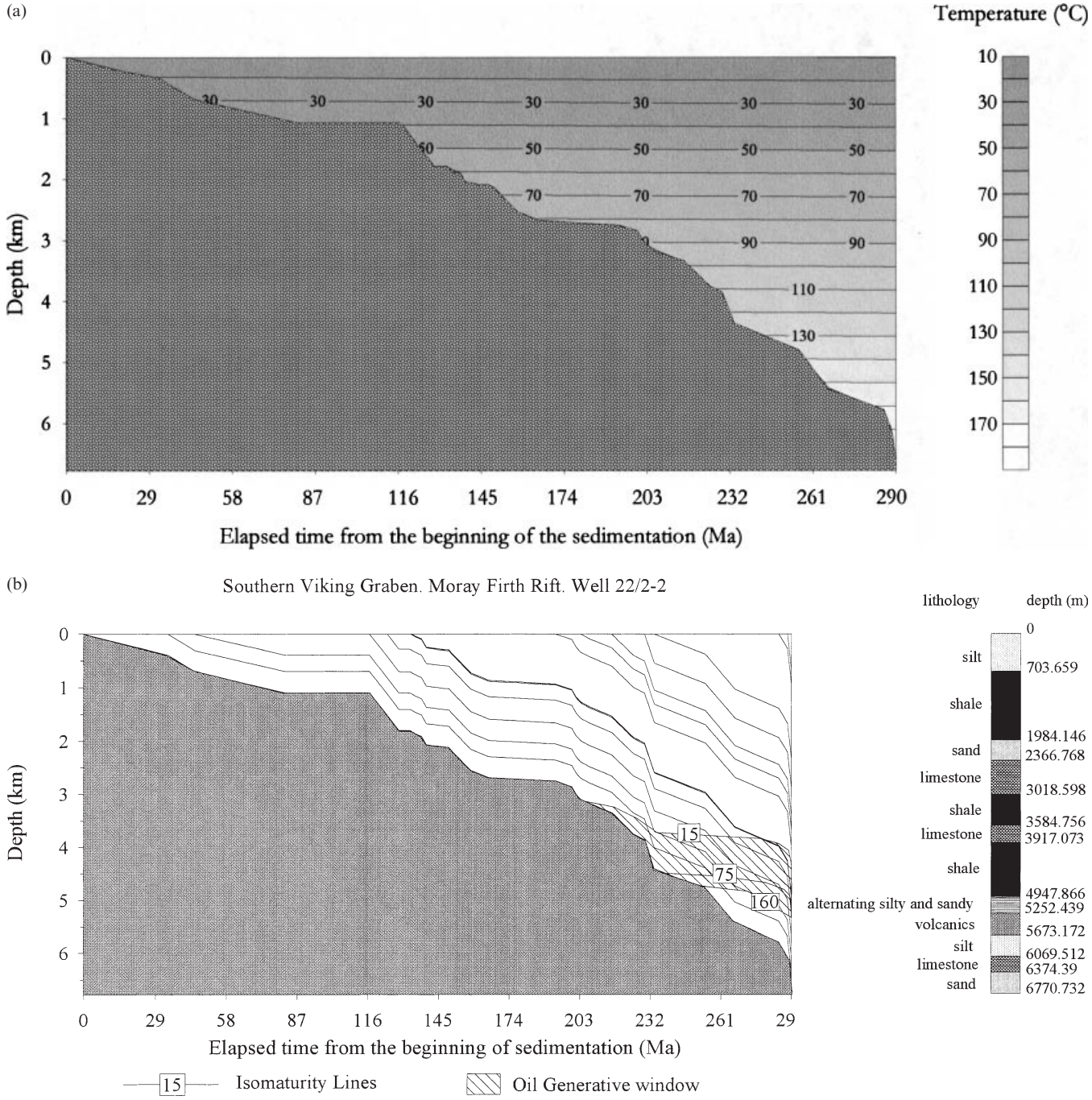

Figure 11. (a) Thermal profile for the 22/2-2 borehole. The x-axis shows the time from the beginning of the sedimentation, and the y-axis shows the depth of the sediments. (b) Maturation history for the 22/2-2 borehole.

From Fig. 11(b) we can draw the following conclusions.

(1) The onset of the maturation, defined by $TTI = 15$ for the basal sediments, occurred at 85.6 Ma BP; the peak of the maturation ($TTI = 75$ for the basal sediments) occurred at 50.33 Ma BP; and the end of the maturation process ($TTI = 160$ for the basal sediments) occurred at 38.6 Ma BP.

(2) At the present time, the predicted depth at which the maturation process is just beginning is 4367 m; the peak of maturation is at 5084 m depth; and the end of the maturation process occurs at 5324 m depth.

These model predictions allow a direct comparison with the results obtained by Goff (1983), who calculated the maturation history using a correlation between calculated maturity and vitrinite reflectance referred to borehole data in the same general area. His predictions of the timing and the depth interval at the present time for oil maturation are as follows:

(1) oil generation from the Kimmeridge clay began between 80 and 65 Ma BP;

(2) peak oil generation occurred between 65 and 40 Ma BP;

(3) oil generation ended between 20 and 40 Ma BP;

(4) the oil generative window at the present time is located between depths of 2550 and 4500 m.

Our model results for the timing of the various phases of oil maturation are therefore in good agreement with Goff's (1983) results, using a borehole in the same general area. However, there is a significant discrepancy in the estimate of the present-day depth of maturation as a result of the different depth of the sediment column in the borehole used here. For example, the boreholes that Goff (1983) used to calibrate his results had a maximum depth of 5300 m, while the borehole that we consider reaches a depth of 6770 m, in an area of intense sedimentation. The discrepancy implies that the rate of sedimentation in individual boreholes can have a significant effect on the predicted maturation depth, even if the timings of onset and cessation of maturation are in reasonable agreement. We would expect this effect in a basin where all areas have experienced a similar tectonic history, but where sedimentation rates vary laterally.

5 CONCLUSIONS

An analytical model has been developed to predict the evolution of the thermal profile as a function of different sedimentation histories within the Earth's crust. The prime applications of this model are the more accurate prediction of the maturation of organic matter in hydrocarbon source rocks, and the reconstruction of thermotectonic events after calibration with such data. The method is based on calculating an analytical solution for the thermal diffusion equation in the cases of (a) instantaneous sedimentation and (b) a continuous sedimentation. The method allowed us to predict and plot the thermal profiles obtained for a range of cases.

A sensitivity analysis was then carried out in order to examine the effects of the main controlling variables on the system. These variables include the thermal diffusivity and the initial geothermal gradient. Of these three variables, the thermal diffusivity has the least effect on the system, although it can be significant in the case of continuous sedimentation.

The results of our model were then compared with those obtained using models assuming a constant geothermal gradient. The clear finding from the results presented here is that we cannot in general accept the assumption of a constant or time-independent geothermal gradient. Therefore, any maturation analysis should explicitly consider the effect of the thermal transient created by the sedimentary blanketing effect.

We conclude with a few important points to emerge from the work.

(1) A detailed knowledge of the lithostratigraphy, and of the thermal conditions in the past, is required to reconstruct and interpret the thermal (and consequently the maturation) history of a sedimentary basin.

(2) A systematic and significant overestimation in the maturation index can result if the time-dependent evolution of the geothermal gradient is neglected.

(3) The best fits of our model, calibrated with present-day maturation data (vitrinite reflectance) could in principle be used to infer the palaeogeothermal gradient.

The model can nevertheless still be improved upon: this is especially important if we want to deal explicitly with the effect of more complicated sedimentary histories, or situations where lateral heat flow is important. This would require recourse to numerical rather than analytical techniques.

ACKNOWLEDGMENTS

The work described above was carried out during an MSc project funded jointly by the British Council and Enterprise Oil Ltd. We are grateful to Jon Turner for access to the borehole data used in the Central North Sea study, for his helpful advice and encouragement in the course of the work, and for his constructive review of the manuscript. We are also grateful to an anonymous reviewer for constructive comments on an earlier draft.

REFERENCES

Birch, F., Roy, R. & Decker, E.R., 1968. Heat Flow and Thermal History in New York and New England, in *Studies of Appalachian Geology: Northern and Maritime,* pp. 437–451, Zen, E., White, W.S., Hadley, J.B. & Thompson, B., Interscience, New York.

Bostick, N.H., 1973. Time as a factor in thermal metamorphism of phytoclasts (coally particles), *7th Cong. Intern. Strat. Geol. Carbonif., Compte Rendu,* **2,** 183–193.

Brigaud, F., Vasseur, G. & Caillet, G., 1994. Thermal state in the North Viking Graben (North Sea) determined from oil exploration well data, *Geophysics,* **57,** 69–88.

Carslaw, H.S. & Jaeger, J.C., 1959. *Conduction of Heat in Solids,* pp. 387–389, Clarendon Press, Oxford.

Cranganu, C. & Deming, D., 1996. Heat Flow and Hydrocarbon Generation in the Transylvanian Basin, Romania, *AAPG Bull.,* **80,** 1641–1653.

Goff, J.C., 1983. Hydrocarbon generation and migration from Jurassic source rocks in the E Shetland Basin and Viking Graben of the Northern North Sea, *J. geol. Soc. Lond.,* **140,** 445–474.

Hood, A., Gutjahr, C.C.M. & Heacock, R.L., 1975. Organic metamorphism at the generation of petroleum, *AAPG Bull.,* **59,** 986–996.

Hunt, J.M., 1995. *Petroleum Geochemistry and Geology,* pp. 141–184, W. H. Freeman & Co., New York.

Karweil, J., 1956. The Coal Metamorphism from the Standpoint of the Physical Chemistry, *Z. Deutscher Geol. Ges.,* **107,** 132–139 (in German).

Lopatin, N.V., 1976. Historico-genetic analysis of petroleum generation: Application of a model of uniform continuous subsidence of the oil-source bed, *AN SSSR Izv. Ser. Geol.,* **8,** 93–101 (in Russian).

McKenzie, D.P., 1978. Some remarks on the development of sedimentary basins, *Earth planet. Sci. Lett.,* **40,** 25–32.

Mongelli, F., 1981. Elementi di Prospezione per L'energia Geotermica, pp. 58–61, Editrice Adriatica, Bari.

Mongelli, F. & Palumbo, F., 1998. 2D and 3D modelling of the thermal evolution of sedimentary basins and their applications, *Presented at the XXIII General Ass. Europ. geophys. Soc.*

North, F.K., 1985. *Petroleum Geology,* pp. 49–68, Allen and Unwin Publishers, Boston.

Oliva, P.R. & Terrasi, F., 1976. *Elaborazione Statistica dei Risultati Sperimentali,* Liguori editore, Napoli.

Pieri, M., 1988. *Petroleum: Origin, Exploration, Exploitation, Statistical Data and Economical Aspects,* pp. 76–87, Zanichelli, Bologna.

Sajgó, C., Horváth, Z.A. & Lefler, J., 1988. An Organic Maturation Study of the Hód-I borehole (Pannonian Basin), *AAPG Mem.,* **45,** 297–309.

Stegena, L., 1988. Palaeogeothermics, in *Handbook of Terrestrial Heat Flow Density Determination,* pp. 391–419, eds Huenel, A., Rybach, C. & Stegena, L., Solid Earth Science Library, Kluwer, Dordrecht.

Stegena, L., Géczi, B. & Horváth, F., 1975. Late Cenozoic evolution of the Pannonian Basin, *Tectonophysics,* **26,** 71–91.

Tissot, B., 1969. Primières données sur le mécanismes et la cinétique de la formation du pétrole dans les sédiments: Simulation d'un schema réactionnel sur ordinateur, *Rev. l'Inst. Français du pétrole,* **24(4),** 470–501.

Vajk, R., 1953. Hungary, in *The Science of Petroleum* (Vol. VI part I), *The World's Oilfields: the Eastern Hemisphere,* pp. 40–42, Illing, V.C., Oxford University Press, Oxford.

Vetö, I. & Dövényi, P., 1986. Methods for paleotemperature estimation using vitrinite reflectance data: a critical evaluation, in *Lecture Notes in Earth Science, Paleogeothermics: Evaluation of Geothermal Conditions in the Geological Past,* **5,** pp. 105–118, eds Bunderbarth, A. & Stegena, L.

Visarion, M., Polonic, P. & Ali-Mehmed, E., 1979. Structural characteristics of the Pannonian Depression (southern sector), resulting from the complex study of geophysical data, *Stud. The. Inst. Geol. (Rom.), Ser. D.,* **12,** 5–18.

Waples, D.W., 1980. Time and temperature in petroleum formation: application of Lopatin method to petroleum exploration, *AAPG Bull.,* **64,** 916–926.